GEOLOGICA CARPATHICA, 54, 2, BRATISLAVA, APRIL 2003
107–118

CALCAREOUS NANNOFOSSIL STRATIGRAPHY OF TERTIARY SUBMARINE FAN DEPOSITS FROM THE KLEMATIA-PARAMYTHIA BASIN (PINDOS FORELAND BASIN, WESTERN GREECE)

KRISTALINA STOYKOVA[1], PAVLOS AVRAMIDIS[2] and ABRAHAM ZELILIDIS[2]

[1]Geological Institute Bulgarian Academy of Sciences, Department of Paleontology and Stratigraphy, BG-1113 Sofia, Bulgaria; stoykova@geology.bas.bg
[2]University of Patras, Department of Geology, Laboratory of Sedimentology, 26500 Patras, Greece; P.Avramidis@upatras.gr, A.Zelilidis@upatras.gr

(Manuscript received July 1, 2002; accepted in revised form December 12, 2002)

Abstract: In the Klematia-Paramythia Basin, which belongs to the middle Ionian zone and is part of the Pindos Foreland Basin, submarine fan deposits accumulated from the Middle Eocene to the Middle Miocene. Calcareous nannofossils are used as a tool for dating and correlation of the fan sediments. Calcareous nannofossil assemblages have been studied in four main geological cross-sections, located in the Pindos Foreland Basin. Seven nannofossil biostratigraphic units were detected — two in the Middle and Upper Eocene (NP16, NP17–20), one in the Lower Oligocene (NP21), one in the Upper Oligocene (NP24–25), two in the Lower Miocene (NN1, NN2–3) and one in the Middle Miocene (NN7). The Upper Miocene NN8–12 interval probably occurs in the section A–A'. These age data indicate that the Pindos foredeep, as a result of Pindos thrust activity, began subsiding during the Middle Eocene. The basin was filled by submarine fan deposits until the Middle (Late?) Miocene, when internal thrusting ended sedimentation.

Key words: Eocene, Oligocene, Miocene, NW Greece, Pindos Foreland Basin, biostratigraphy, calcareous nannofossils.

Introduction and geological setting

The study area, located in northwestern Greece, is a part of the external Hellenides and belongs to the Pindos Foreland Basin of the Hellenide orogen. The basin is filled by submarine fan deposits and is segmented during its evolution by thrusting and strike-slip motions (Fig. 1).

The Pindos Foreland Basin (Underhill 1989; Clews 1989; Leigh & Hartley 1992; Avramidis 1999; Avramidis et al. 2000) comprises the Gavrovo and the Ionian geotectonic zones sensu Aubouin (1965). The studied area is part of the Ionian Zone, which due to the differentiation of the carbonate facies, the flysch (turbidite) deposits and the existence of the internal thrusting, is subdivided from east to west in the internal, middle and external Ionian zones (IGSR & IFP 1966) (Fig. 1). The subdivision of the Ionian Zone occurred during Late Oligocene to Early Miocene.

The evolution of the Pindos Foreland Basin was mainly influenced by the activity of the Pindos and Ionian thrusts, and secondarily by the Gavrovo thrust and internal thrusts of the Ionian Zone (Fig. 1). Due to the Pindos thrust activity a foredeep was formed during Middle Eocene (IGSR & IFP 1966), whereas due to the internal thrusting the foreland changed to a complex type foreland basin, during the Late Oligocene in its northern part (studied area — Avramidis et al. 2000), and to a piggy back basin, during Early Pliocene in its southern part (Zakynthos area — Zelilidis et al. 1998). The Pindos foredeep during the Middle Eocene was an example of an undefiled foreland basin and these conditions can be related to narrow linear basins where submarine fans accumulated (Avramidis & Zelilidis 2001). The distribution of submarine fan facies was influenced mainly by tectonically driven subsidence and to a lesser degree by sea-level variations (Avramidis et al. 2002).

The objectives of the present paper are to correlate and compare stratigraphical data, obtained from the study of calcareous nannofossils from the turbidites in order to estimate the timing of the major events, which influenced the evolution of the Pindos Foreland Basin.

P. Avramidis and A. Zelilidis (University of Patras, Greece) carried out all field studies, sedimentological and tectonic interpretations. K. Stoykova (Geological Institute, Sofia) performed calcareous nannofossil studies and the biostratigraphic interpretation of the obtained data.

Depositional environments

The Pindos Foreland Basin consists of several thousand metres thick flysch sequences (submarine fans). Their tectonically controlled deposition took place during the westward progradation of the external Hellenides and extended longitudinally to the axes of the synclines that formed during this deformation (Fig. 1). The source material of the submarine fans was mainly within the Pindos Mountains (Piper et al. 1978; Faupl et al. 1998; Avramidis & Zelilidis 2001).

A number of researchers have interpreted the flysch of the Pindos foreland as parts of a submarine fan (turbidite deposits) (Piper et al. 1978; Clews 1989; Wilpshaar 1995; Avramidis & Kontopoulos 1998; Avramidis & Zelilidis 1998; Avramidis et

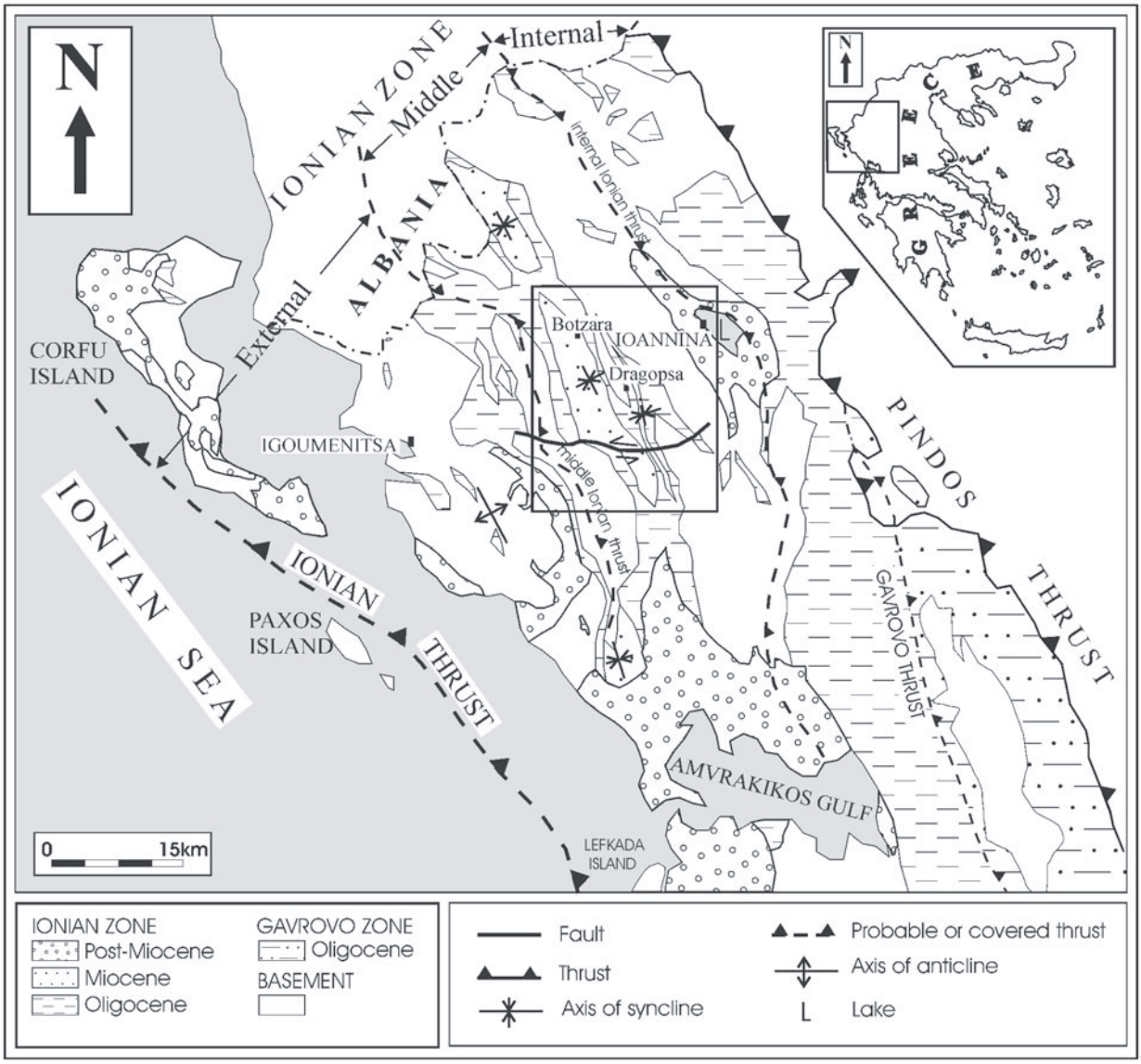

Fig. 1. Simplified geological map of western Greece, showing the Ionian and Gavrovo Zones (after Avramidis et al. 2000) and the location of the studied basin.

al. 2000). Adjacent to the Pindos thrust front (internal Ionian zone — in the north and Gavrovo Zone — in the south, Fig. 1) coarse-grained sediments were deposited, representing the proximal part of a submarine fan, while westward (middle and external Ionian zone), fine-grained sediments accumulated representing the distal parts of the fan (Fig. 1).

Flysch deposits usually overlie conformably the Eocene limestones, but there are some places, where their contact is marked by an unconformity. The age of the onset of flysch sedimentation in the Pindos Foreland Basin is a controversial point. I.G.S.R & I.F.P. (1966) proposed that the onset of flysch sedimentation took place in the Late Eocene, while Fleury (1980), Leigh & Hartley (1991), Wilpshaar (1995) and Bellas (1997) proposed an Early Oligocene age. In contrast to the above studies, B.P. (1971) proposed an Early to Middle Miocene age for the onset of flysch sedimentation, an age which has not been widely accepted.

Avramidis et al. (2000), studying the turbidite deposits in the middle Ionian zone, interpreted them as submarine fan deposits and classified them with the main facies types and facies association of turbidite depositional environments (Mutti & Ricci Lucchi 1972, 1975; Walker 1978). The Middle Eocene to Upper Oligocene turbidite sediments, deposited in the middle Ionian zone, represent the distal parts of a submarine fan (lobe, lobe-fringe and basin plain), while the Lower to Upper Miocene turbidite sediments, due to differential tectonic evolution of Pindos Foreland Basin, represent both proximal and distal depositional facies of inner and outer submarine fans. According to Avramidis et al. (2000) the Middle Eocene to Upper Oligocene formations of turbidites are up to 1050 m thick and were deposited before the division of the Ionian Zone. The Lower Miocene to Upper Miocene turbidites were deposited after the segmentation of the Ionian Zone within a restricted basin, and are up to 2300 m thick.

In the middle Ionian zone, the major thickness of submarine fan deposits (up to 3300 m thick) is present in the Klematia-Paramythia Basin. The Klematia-Paramythia Basin involves the Botzara and Dragopsa synclines and their deposits were examined in four geological cross-sections (Fig. 2).

Section A–A' has a total stratigraphic thickness of up to 3300 m. From the base to the top it consists of outer fan deposits (up to 800 m), basin plain deposits (up to150 m), inner fan deposits (up to 90 m) and outer fan deposits (up to 2260 m) (Fig. 3). A total of 16 samples have been examined for calcareous nannofossils.

Eastern part of Botzara syncline. This section has a thickness of up to 1250 m and consists of outer fan (up to 450 m) and inner fan deposits (up to 800 m). Three samples were examined from the outer fan deposits (FL1, FL2 and FL7) and three samples from the inner fan deposits (MI1, MI6 and MI 11) (Fig. 4).

Section B–B'. It is up to 1720 m thick and from the base upward consists of outer fan deposits (up to 646 m) and inner fan deposits (up to 1074 m). From outer fan deposits three samples were examined (P1, P5 and P7) and from the inner fan — four samples (P8, P9, P12 and P13) (Fig. 5).

Section C–C' has a stratigraphic thickness of up to 360 m and from the base upward consists of basin plain (up to 50 m) and outer fan deposits (up to 310 m). One sample was examined from the basin plain (D2) and three samples from the outer fan deposits (D8, D12 and D13) (Fig. 6).

Calcareous nannofossils — material and methods

Our calcareous nannofossil study is based on 33 samples, taken from the different sections (A–A' — 16 samples, Eastern part of Botzara syncline — 6 samples, B–B' — 7 samples, C–C' — 4 samples — Fig. 2). All samples were processed and the smear-slides were prepared without centrifuging in order to avoid changes in the composition of the original assemblages. A biostratigraphic evaluation was conducted under the light microscope with 1250× magnification. Each slide was observed in normal and cross-polarized light. Most samples were logged two or three times for an average of 40–60 minutes. Some critical samples were examined for several hours. Semi-quantitative analysis has been performed on each sample. The relative abundance of nannofossils was determined in the following way: the species was termed "abundant" if more than 10 specimens can be observed per field of view, "common" (9–2 spec./f.v.) and "rare" (< 2 spec./f.v.).

Calcareous nannofossils are common and moderately well preserved throughout the sections. Only a few samples (4) are devoid of nannofossils. Because of the turbiditic depositional environment, reworking of the nannofossils is commonly observed, as indicated by the presence of many Upper Cretaceous, Paleocene and Lower Eocene species.

Our biostratigraphic interpretations are based on precise determination of the first (FO) and last (LO) occurrences of stratigraphically important nannofossil species, including zonal markers and taxa with well-known stratigraphic range, as well as on careful taxonomic identification of the nannofossils. We tried to use generally accepted taxonomic concepts,

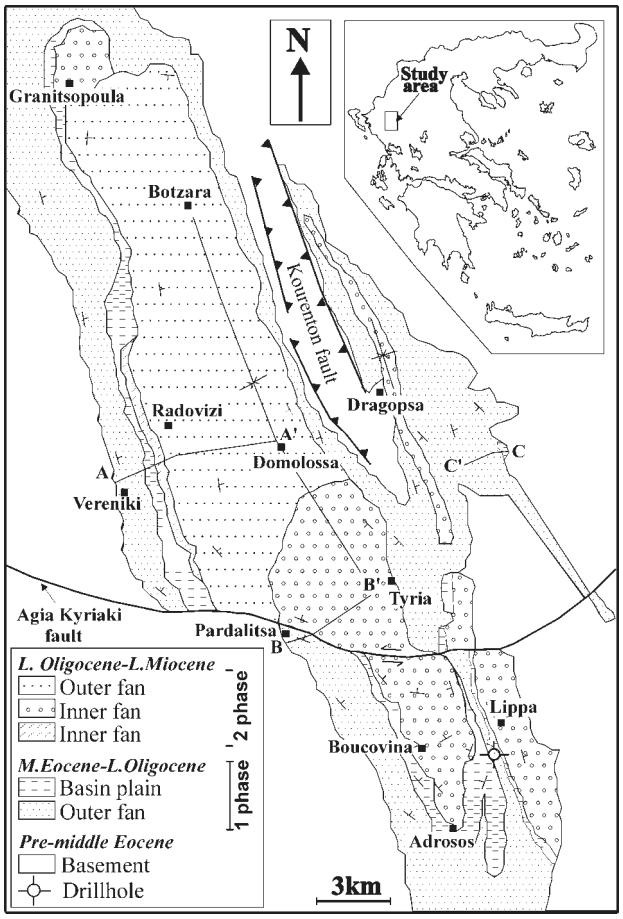

Fig. 2. Geological map, showing the turbidite sub-environment distribution within the Klematia-Paramythia Basin and the position of the sections studied.

following Aubry (1984, 1988, 1989, 1990) and Perch-Nielsen (1985).

In order to achieve an accurate biostratigraphic correlation between the studied sections, we used the standard zonation of Martini (1971). Special attention was paid to samples within important stratigraphic intervals, especially around zonal boundaries. All observations were made on dense smear slides, in order to register the occurrences of rare species. Several of the important boundary markers were absent or scarce in the studied samples. Then in most cases we used combined range of recorded taxa. A calcareous nannofossil range chart is produced for each of the sections studied (Figs. 3–6).

Biostratigraphy

Section A–A'

The section is situated in the central part of the basin (Fig. 2). The thickness of the exposed sediments (turbidites) is up to 3300 m. Stratigraphically the section spans from the Lower Oligocene NP21 Zone up to the Upper Miocene NN8–12 zones. Sixteen samples were investigated, only one containing a poor nannofossil assemblage (M38).

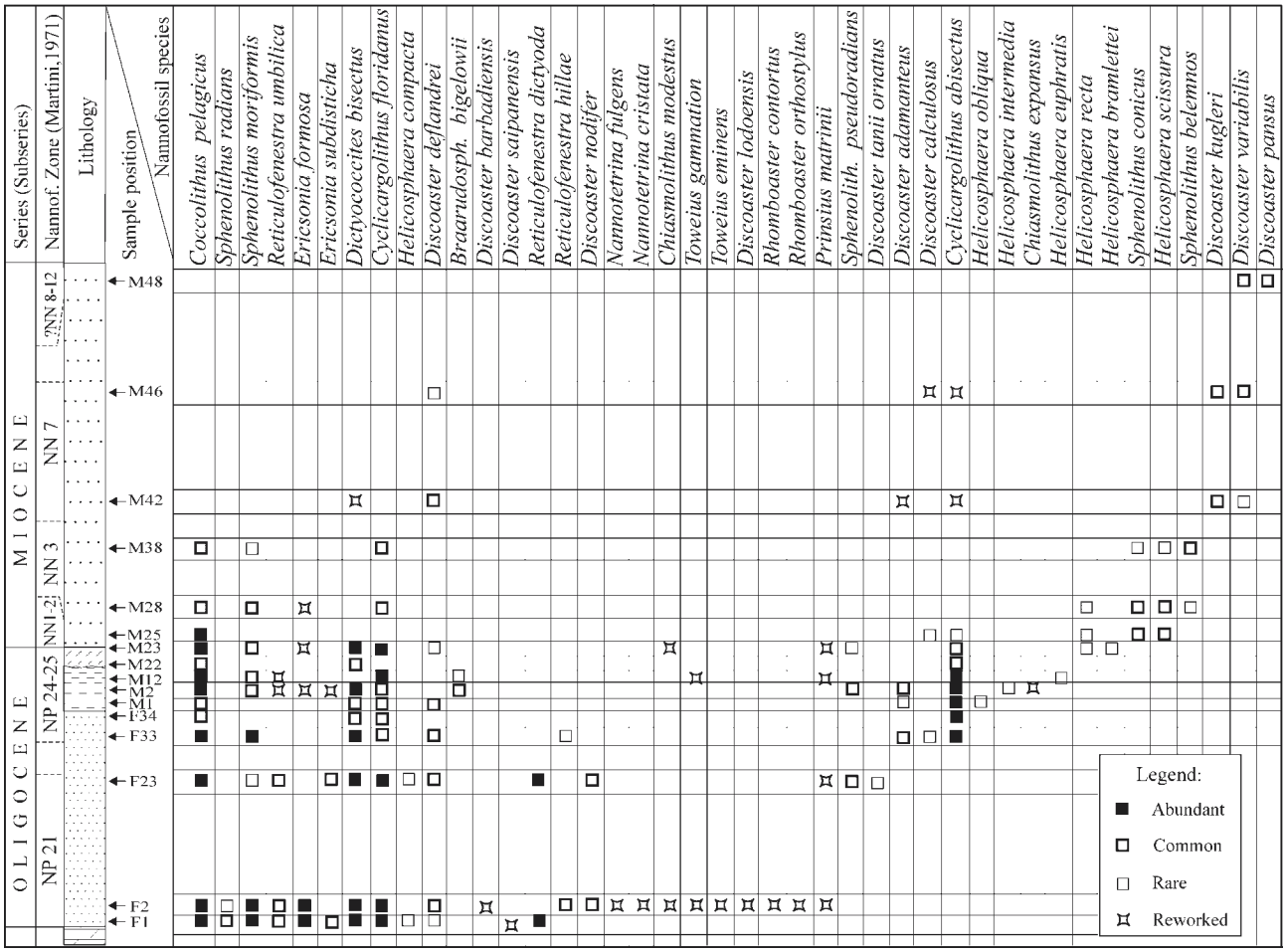

Fig. 3. Range chart of calcareous nannofossils and stratigraphic subdivision of section A–A'.

Notably, it was only in this section that we observed the presence of the nannofossil genera *Braarudosphaera* and *Pontosphaera*, regarded as indicators of a shallow depth of deposition — shelf or hemipelagic environments (Bramlette & Sullivan 1961). Relatively large-sized forms of *Braarudosphaera bigelowii* (Fig. 8.14) are recorded in samples M2 and M12, in the Upper Oligocene zones NP24–25. *Pontosphaera* sp. (Fig. 7.13) is determined in sample M44, in the Middle Miocene Zone NN7.

The occurrence of the recognized calcareous nannofossil species is reported on Fig. 3.

Lower Oligocene, NP21 Ericsonia subdisticha Zone. According to its definition (Roth & Hay 1967 emend. Martini 1970), the zone spans the interval from the LO of *Discoaster saipanensis* to the LO of *Ericsonia formosa*. The lower part of A–A' section is assigned to NP21. The nannofossil assemblage of this zone is dominated by *Ericsonia formosa* (Fig. 7.9), *E. subdisticha* (Fig. 7.3b,4), *Dictyococcites bisectus* (Fig. 7.2,3a,17), *Coccolithus pelagicus*, *Cyclicargolithus floridanus* (Fig. 7.18), *Reticulofenestra dictyoda* and *Sphenolithus moriformis*. Several species are common in this zone: *Reticulofenestra umbilica* (Fig. 7.5,6), *Discoaster deflandrei*, *Discoaster nodifer*, *Sphenolithus pseudoradians*.

The two basal samples of the section (F1, F2), contain a large number of reworked Eocene species such as: *Rhomboaster contortus*, *R. orthostylus*, *Discoaster lodoensis*, *D. saipanensis*, *Toweius eminens*, *T. gammation*, *Chiasmolithus modestus*, *Nannotetrina cristata*, *N. fulgens*.

Because of the uncertainty of reworking in the turbidite deposits, the LO *Ericsonia formosa* could not be used as a reliable datum for the upper boundary of the zone. Therefore it is drawn above the sample F23, by the first occurrence of *Cyclicargolithus abisectus*, *Discoaster adamanteus* and *Discoaster calculosus* in sample F33.

Upper Oligocene, NP24–25 Sphenolithus distentus–Sphenolithus ciperoensis zones. These two zones span the Upper Oligocene and could not be separated because of the scarcity of sphenoliths in this part of the section. The age assignment of the samples F33, F34, M1 to M23 to NP24–25 zones is based on the combined range of the detected species. The lower boundary of the zone is traced by the FO of *Cyclicargolithus abisectus* (Fig. 7.19), *Discoaster adamanteus* (Fig. 9.1) and *Discoaster calculosus*. For the upper boundary (which is the Oligocene/Miocene boundary as well), the LO of *Dictyococcites bisectus* and *Sphenolithus pseudoradians* and/or the FO of *Sphenolithus conicus* and *Helicosphaera scissura* is used for approximation.

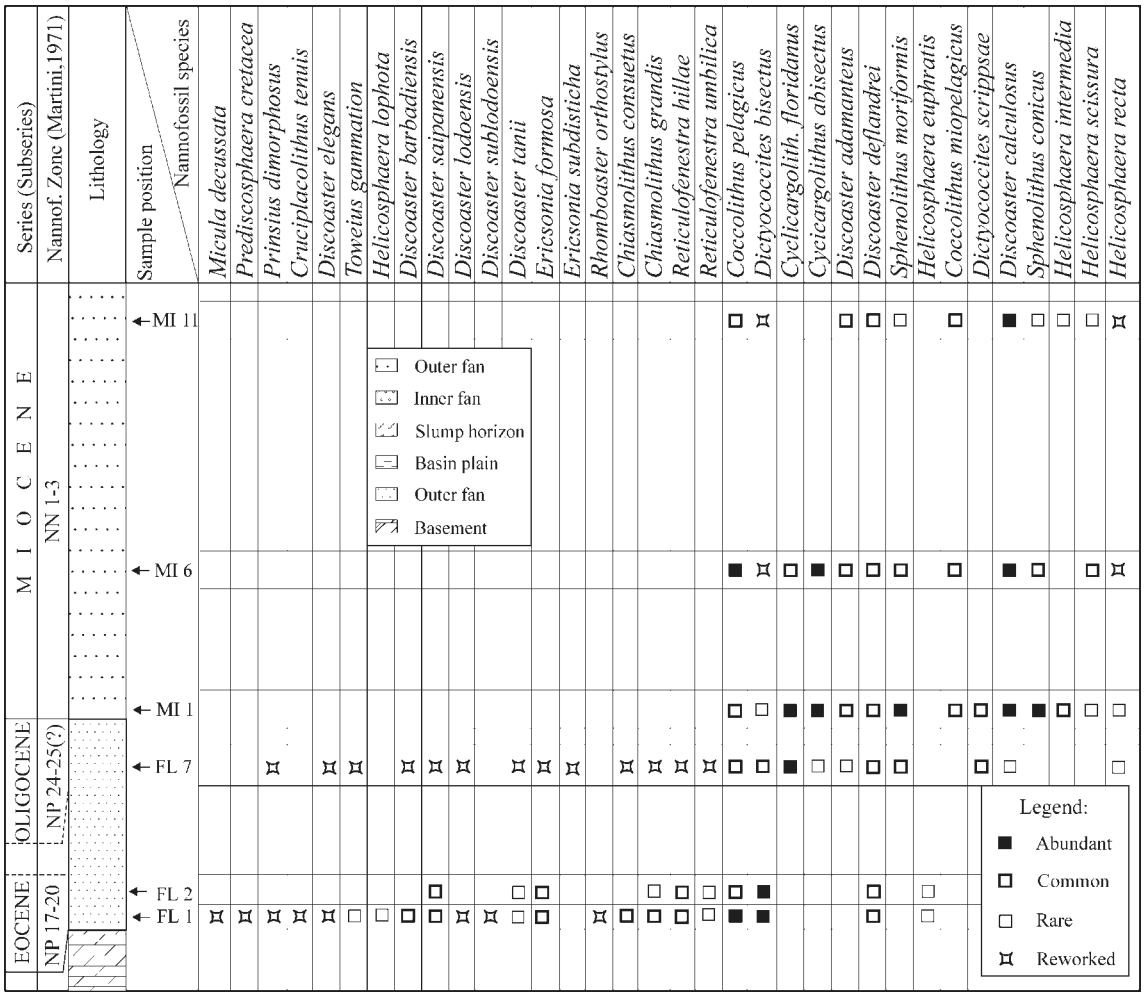

Fig. 4. Range chart of calcareous nannofossils and stratigraphic subdivision of the section E-part of Botzara syncline.

Lower Miocene, NN1–2 T. carinatus-Discoaster druggi zones. The presence of these basal Miocene zones is proven in the middle part of the section, in sample M25. The distinguishing criteria for its lower boundary were stated above in the previous zone. The FO of *Sphenolithus belemnos* is an important nannofossil event, largely used for correlation. This event marks the upper boundary of the zone in our A–A' section, which is drawn between the samples M25 and M28 (Fig. 3).

NN3 S. belemnos Zone. This zone was originally defined as an interval between the LO of *Triquetrorhabdulus carinatus* and the LO of *S. belemnos* (Bramlette et Wilcoxon, 1967). Since *Triquetrorhabdulus carinatus* was not found in our materials, we used the FO of *S. belemnos* as an approximation of the lower boundary and its LO for the upper boundary. Practically, in this section the zone equates with the total range of *S. belemnos*.

Coccolithus pelagicus, *Cyclicargolithus floridanus* and *Helicosphaera scissura* dominate the nannofossil assemblages of the zone.

The upper boundary of NN3 Zone falls between the samples M38 and M42.

Middle Miocene, NN7 Discoaster kugleri Zone. This Middle Miocene zone is located in the upper part of the section (samples M42, M46 — Fig. 3). It is identified by the presence of *Discoaster kugleri*. The total range of this species defines the lower and upper boundary of the zone. *Discoaster deflandrei* and *Discoaster variabilis* are common taxa. Small, difficult to determination reticulofenestrids are observed in the zone.

? NN8–12 zones. The questionable presence of these Upper Miocene zones in the topmost sample of the section (M48) is based on the common occurrence of *Discoaster pansus* (Fig. 9.5,6). According to Perch-Nielsen (1985) its range is NN12–NN15, and our initial age-estimation was the NN12 Zone. Aubry (1984, p. 155) in her comprehensive book on *Discoaster* stated that "Its FO is later than for *D. variabilis* and before *D. decorus*", that is the FO of *D. pansus* is not a precisely fixed event, but occurred in a large stratigraphic interval — NN6 to NN15. Therefore it cannot be used for a precise age determination.

Section in the eastern part of the Botzara syncline

The section is located in the northern parts of the basin and comprises up to 1250 m a turbiditic succession up to 1250 m thick (Fig. 2). Middle-Upper Eocene (NP17–20) to Lower Miocene (NN1–3) sediments are exposed in this sec-

tion. Six samples were studied, all displaying good preservation of the calcareous nannofossil assemblages (Fig. 4).

Middle–Upper Eocene, NP17–20 Discoaster saipanensis–Sphenolithus pseudoradians zones. The lower part of the section (samples FL1 and FL2) is assigned to this large stratigraphic interval, because we did not find any of the marker species *Chiasmolithus oamaruensis*, *Isthmolithus recurvus* and *Sphenolithus pseudoradians*. Instead, we recorded a moderately rich species association with common *Dictyococcites bisectus*, *Reticulofenestra umbilica* (Fig. 7.7), *R. hillae* (Fig. 7.8), *Cribrocentrum reticulatum* (Fig. 7.1), *Discoaster barbadiensis*, *D. saipanensis* (Fig. 4). The first two species have their FO within the NP17 Zone, whereas the last two have their LO at the top of the NP20 Zone. For this reason we infer the NP17–20 zones for these samples. We avoid using the LO of *Chiasmolithus grandis* (Fig. 8.16) as an event marking the top of NP17, supposing it might be easily reworked.

Upper Oligocene, NP24–25 Sphenolithus distentus–Sphenolithus ciperoensis zones. These zones are inferred for sample FL7. It is proven by the FO of *Cyclicargolithus abisectus*, *Helicosphaera recta*, *Discoaster calculosus* and *D. adamanteus*. The nannofossil association is similar to that observed in A–A' section (see Fig. 4 for details). The upper zonal boundary is placed between the samples FL7 and MI1, at the FO of *Sphenolithus conicus* and *Helicosphaera scissura* in MI1.

Lower Miocene, NN1–3 T. carinatus–S. belemnos zones. These zones span the middle and upper part of the section (samples MI1 to MI11, Fig. 4). The recognition is based on the occurrence of *Sphenolithus conicus*, ranging from NN1 to NN3, as well as the presence of abundant Early Miocene nannofossil species such as *Helicosphaera scissura*, *H. intermedia* (Fig. 7.14), *Coccolithus pelagicus*, *C. miopelagicus*.

Section B–B'

This section is located in the western part of the Botzara syncline, in the southern part of the basin (Fig. 2). The succession of calcareous nannofossil zones established and their vertical distribution is reported in Fig. 5. The succession covers a large stratigraphic interval — from the Middle-Upper Eocene (NP17–20 zones) to the Middle Miocene (NN7 Zone) and is up to 1720 m thick.

Middle–Upper Eocene, NP17–20 Discoaster saipanensis–Sphenolithus pseudoradians zones. These zones are recognized in the base of the section, in sample P1 (Fig. 5). The nannofossil association is rich and diverse, dominated by *Dic-*

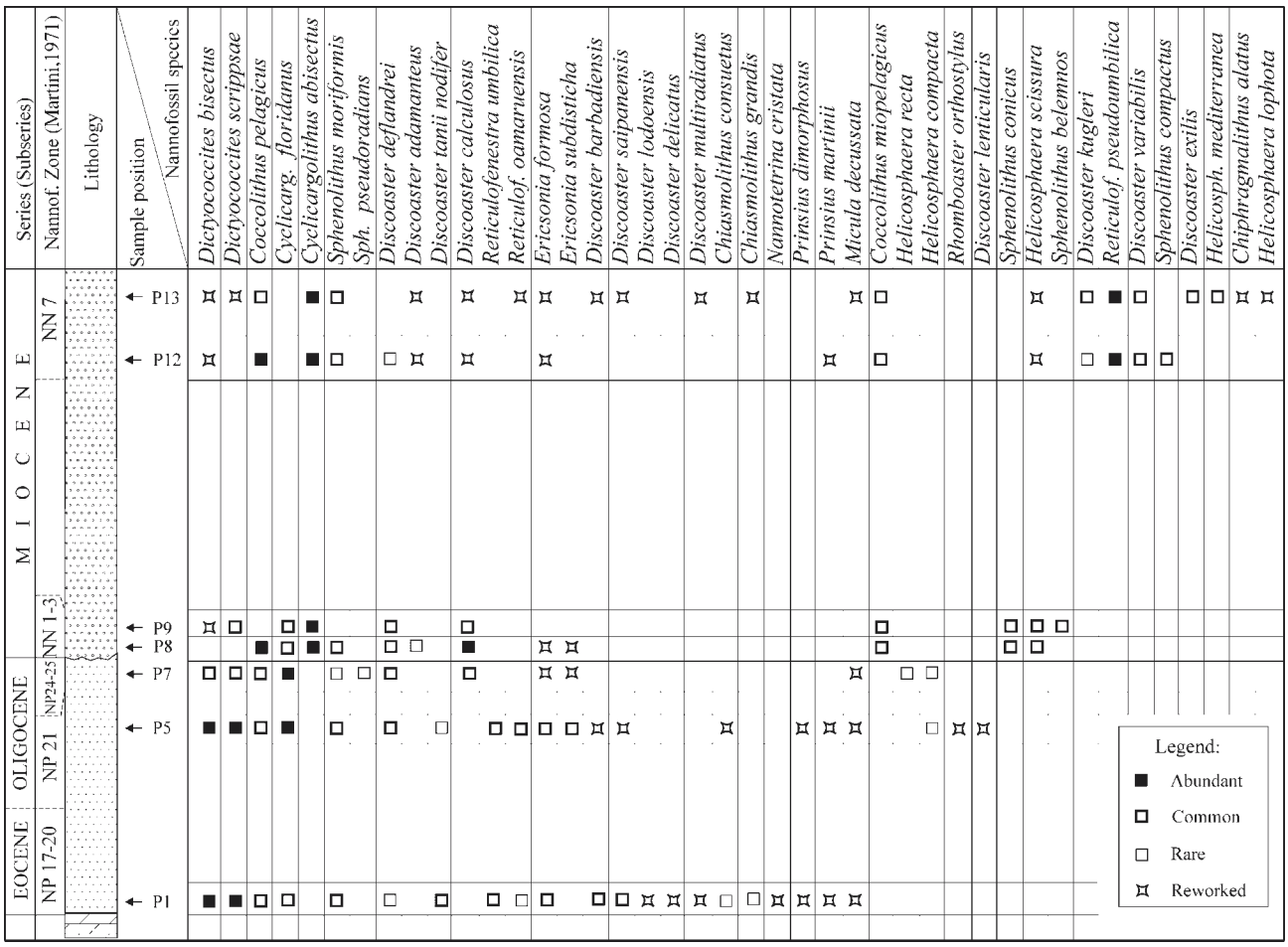

Fig. 5. Range chart of calcareous nannofossils and stratigraphic subdivision of section B–B'.

tyococcites bisectus and *D. scrippsae*. It is similar to the association of the same zone, recorded in the Eastern part of the Botzara Section. The FO of *Ericsonia subdisticha* in the sample P5 marks the upper boundary of the zone.

Lower Oligocene, NP21 Ericsonia subdisticha Zone. This zone is recorded in sample P5. Its lower boundary is drawn by the FO *Ericsonia subdisticha* (Fig. 7.4) — a species, which occurs commonly in NP21 only.

Upper Oligocene, NP24–25 Sphenolithus distentus–Sphenolithus ciperoensis zones. These zones are identified by the co-occurrence of *Helicosphaera recta* (Fig. 7.15) and *Discoaster calculosus* in sample P7. The nannofossil association is analogous to those observed in A–A' and in the Eastern part of the Botzara sections.

Lower Miocene, NN1–3 T. carinatus–S. belemnos zones. The lower boundary is fixed at the FO of *Sphenolithus conicus* and *Helicosphaera scissura* (by analogy with A–A' and the E-part of the Botzara sections) between the samples P7 and P8 (Fig. 5). The upper boundary is marked by the LO of *Sphenolithus belemnos* and *S. conicus*. It is traced above the sample P9. Typical Lower Miocene association, containing *Discoaster calculosus*, *Cyclicargolithus abisectus*, *Coccolithus pelagicus*, *C. miopelagicus*, *Sphenolithus conicus* and *Helicosphaera scissura* is documented from the samples P8 and P9.

Middle Miocene, NN7 Discoaster kugleri Zone. The zone is distinguished in the upper part of the section (samples P12, P13 — Fig. 5). It is based on the total range of its index-species, *Discoaster kugleri*. Small-sized reticulofenestrids (mainly *Reticulofenestra pseudoumbilica*) dominate the nannofossil associations of this zone. *Discoaster variabilis*, *D. exilis* and *Coccolithus pelagicus–C. miopelagicus* occur commonly.

Section C–C'

The section is situated in the Dragopsa syncline, at the eastern margin of the basin (Fig. 2). The thickness of the sediments is relatively small — up to 360 m, due to the incompleteness of the section. Middle Eocene (NP16), Upper Eocene (NP17–20) and Lower Miocene (NN1–3 zones) has been proven (Fig. 6). The whole Oligocene is missing in this location.

Middle Eocene, NP16 Discoaster tanii nodifer Zone. This is the oldest zone recognized in this study. Its presence in sample D2 is undoubtedly proven by the co-occurrence of *Discoaster bifax* and *Chiasmolithus modestus*, ranging only in the NP16 Zone. An additional argument for this age determination is the occurrence of *Nannotetrina cristata* (Fig. 9.8), *Chiasmolithus solitus* and *Ch. expansus* (Fig. 8.3), which has its LO at the top of NP16 (Fig. 6).

Middle–Upper Eocene, NP17–20 Discoaster saipanensis–Sphenolithus pseudoradians zones. These zones are based on the rich and various nannofossil association, observed in sample D8. The lower boundary is approximated by the FOs of *Discoaster tanii nodifer*, *Dicyococcites bisectus*, *D. scrippsae* and *Helicosphaera compacta* (Fig. 8.1).

There appears to be an unconformity at the top of this zone, as indicated from the overlying Lower Miocene sediments.

Lower Miocene, NN1–3 T. carinatus–S. belemnos zones. These zones are recognized in the samples D12 and D13. They are based on the total range of *Sphenolithus conicus*. The nannofossil assemblages are abundant, dominated by *S. conicus*, *Cyclicargolithus floridanus*, *C. abisectus*. Reworking of Eocene species from the underlying sediments is noticeable in D12 sample.

Conclusions

A relatively expanded Middle Eocene to Middle (Upper?) Miocene turbiditic sequence was recovered from the studied area (Pindos Foreland Basin, NW Greece), indicating that the Pindos foredeep was filled from the Middle Eocene onwards. Calcareous nannofossils are moderately well preserved and

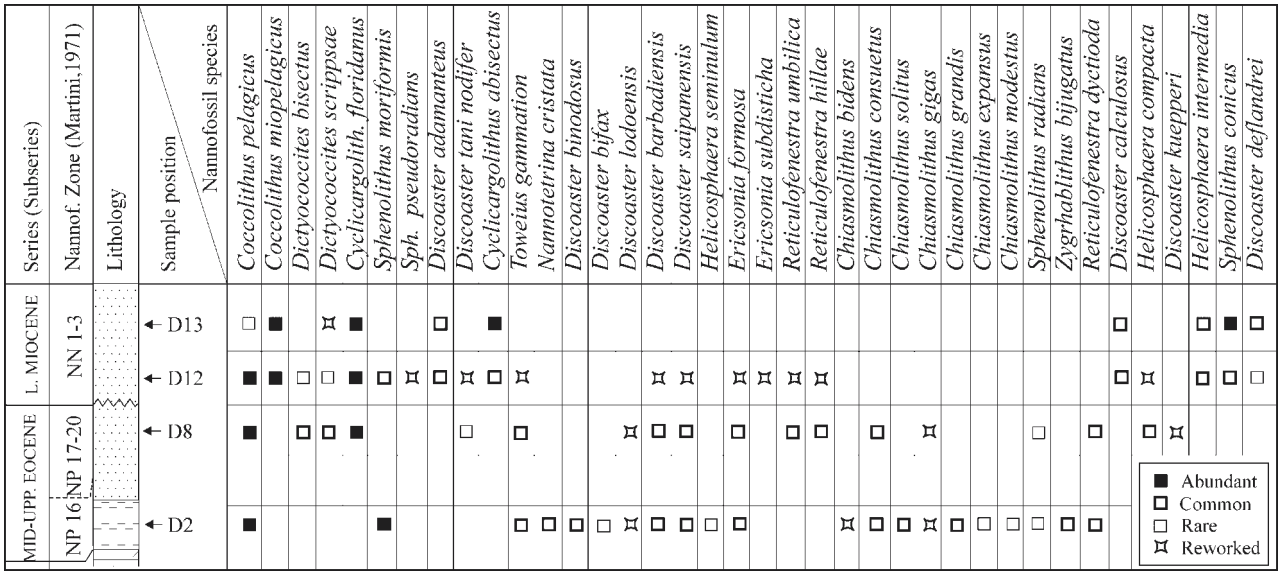

Fig. 6. Range chart of calcareous nannofossils and stratigraphic subdivision of section C–C'.

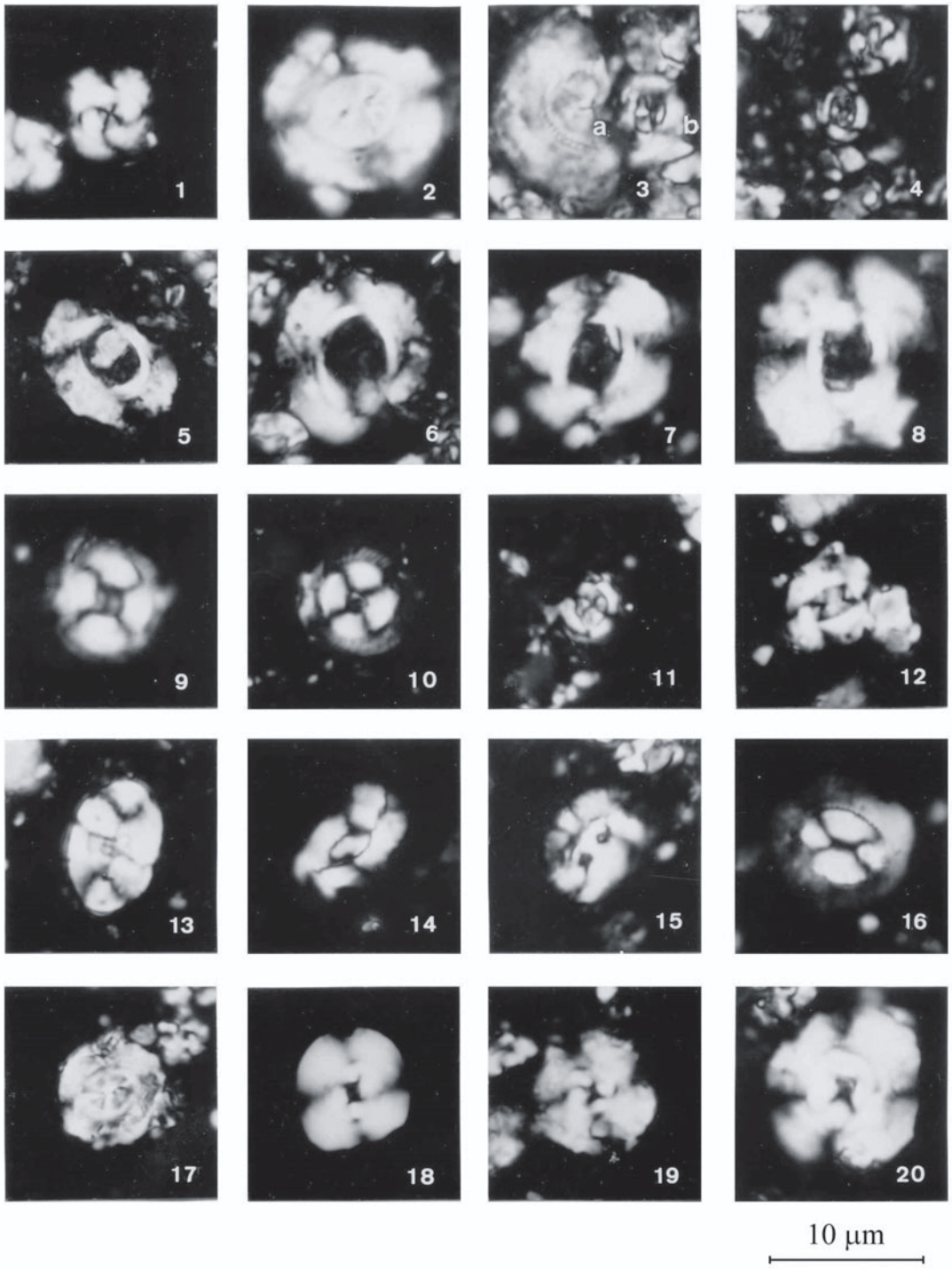

Fig. 7. LM microphotographs of calcareous nannofossil taxa from the studied sections, all pictures with crossed nicols, scale bar — 10 μm: **1.** *Cribrocentrum reticulatum* (Gartner et Smith) Perch-Nielsen, sample FL1, section E-part of Botzara syncline. **2, 3a.** *Dictyococcites bisectus* (Hay, Mohler et Wade) Bukry et Percival, sample F1, section A–A'. **3b, 4.** *Ericsonia subdisticha* (Roth et Hay) Roth; 3b — sample F1, section A–A'; 4 — sample P5, section B–B'. **5–7.** *Reticulofenestra umbilica* (Levin) Martini et Ritzkowski; 5 — sample F2; 6 — sample F23, section A–A'; 7 — sample FL2, section E-part of Botzara syncline. **8.** *Reticulofenestra hillae* Bukry et Percival, sample FL1, section E-part of Botzara syncline. **9–10.** *Ericsonia formosa* (Kamptner) Haq; 9 — sample F2, section A–A'; 10 — sample P5, section B–B'. **11.** *Ericsonia subdisticha* (Roth et Hay) Roth, sample F2, section A–A'. **12.** *Reticulofenestra oamaruensis* (Deflandre) Stradner, sample P5, section B–B'. **13.** *Ponthosphaera* sp., sample M44, section A–A'. **14.** *Helicosphaera intermedia* Martini, sample MI1, section E-part of Botzara syncline. **15.** *Helicosphaera recta* (Haq) Jafar et Martini, sample P7, section B–B'. **16.** *Coccolithus pelagicus* (Wallich) Schiller, sample M23, section A–A'. **17.** *Dictyococcites bisectus* (Hay, Mohler et Wade) Bukry et Percival, sample P5, section B–B'. **18.** *Cyclicargolithus floridanus* (Roth et Hay) Bukry, sample FL1, section E-part of Botzara syncline. **19–20.** *Cyclicargolithus abisectus* (Muller) Wise; 19 — sample F33; 20 — sample M42, section A–A'.

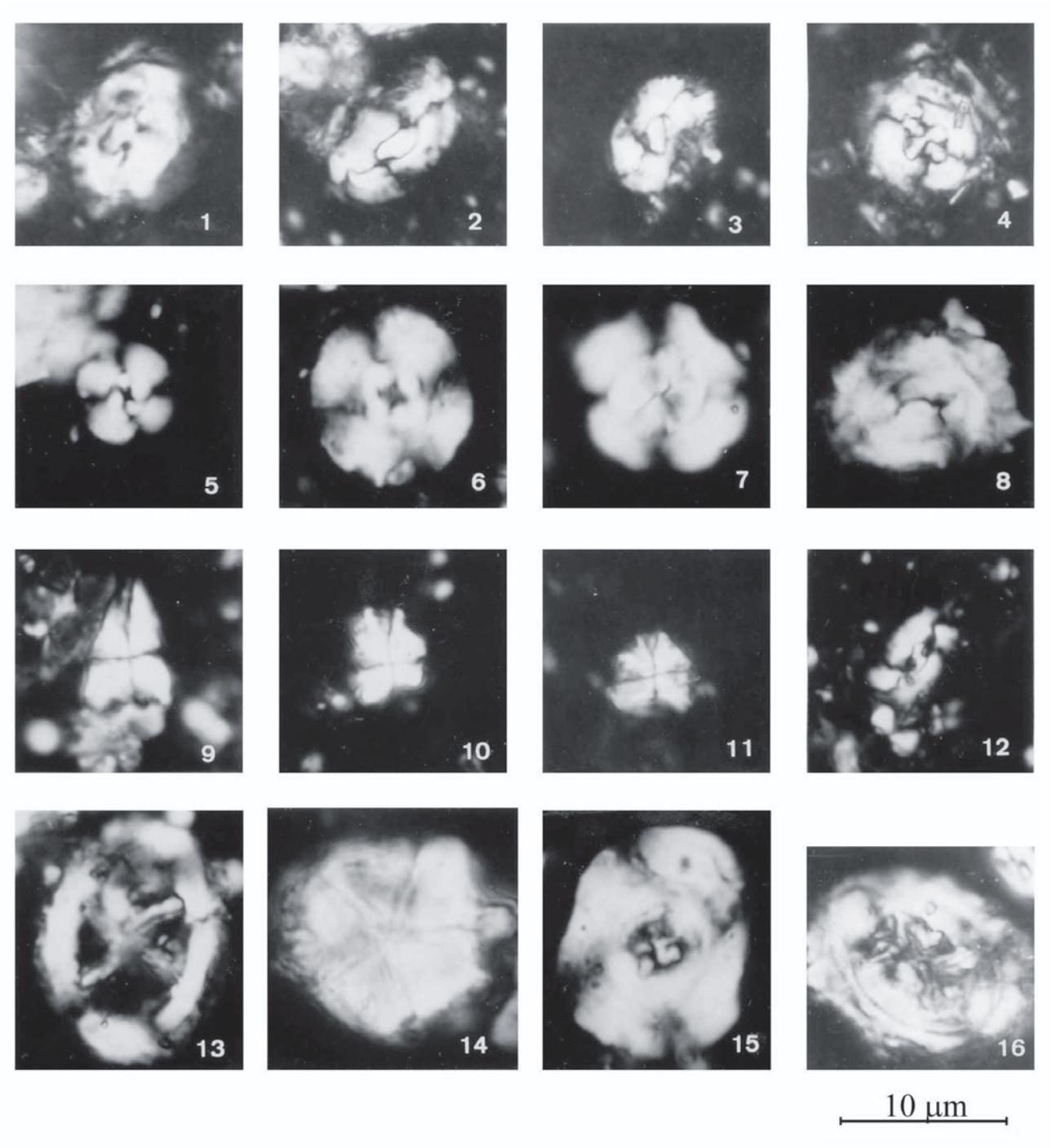

Fig. 8. LM microphotographs of calcareous nannofossil taxa from the studied sections, all pictures with crossed nicols, scale bar — 10 µm: **1.** *Helicosphaera compacta* Bramlette et Wilcoxon, sample D8, section C–C'. **2.** *Helicosphaera euphratis* Haq, sample FL1, section E-part of Botzara syncline. **3.** *Helicosphaera lophota* Bramlette et Sullivan, sample FL1, section E-part of Botzara syncline. **4.** *Chiasmolithus consuetus* (Bramlette et Sullivan) Hay et Mohler, sample P1, section B–B'. **5–6.** *Cyclicargolithus floridanus* (Roth et Hay) Bukry; 5 — sample P5, section B–B'; 6 — sample M2, section A–A'. **7.** *Dictyococcites bisectus* (Hay, Mohler et Wade) Bukry et Percival, sample M2, section A–A'. **8.** *Coccolithus pelagicus* (Wallich) Schiller, sample M25, section A–A'. **9.** *Sphenolithus editus* Perch-Nielsen, sample M2, section A–A', reworked from the Lower Eocene. **10.** *Sphenolithus capricornutus* Bukry et Percival, sample M28, section A–A'. **11.** *Sphenolithus moriformis* (Bronnimann et Stradner) Bramlette et Wilcoxon, sample MI1, section E-part of Botzara syncline. **12.** *Helicosphaera intermedia* Martini, sample M2, section A–A'. **13.** *Chiasmolithus expansus* (Bramlette et Sullivan) Gartner, sample D2, section C–C'. **14.** *Braarudosphaera bigelowii* (Gran et Braarud) Deflandre, sample M2, section A–A'. **15.** *Reticulofenestra* sp. ex gr. *umbilica*, sample P1, section B–B'. **16.** *Chiasmolithus grandis* (Bramlette et Riedel) Radomski, sample FL2, section E-part of Botzara syncline.

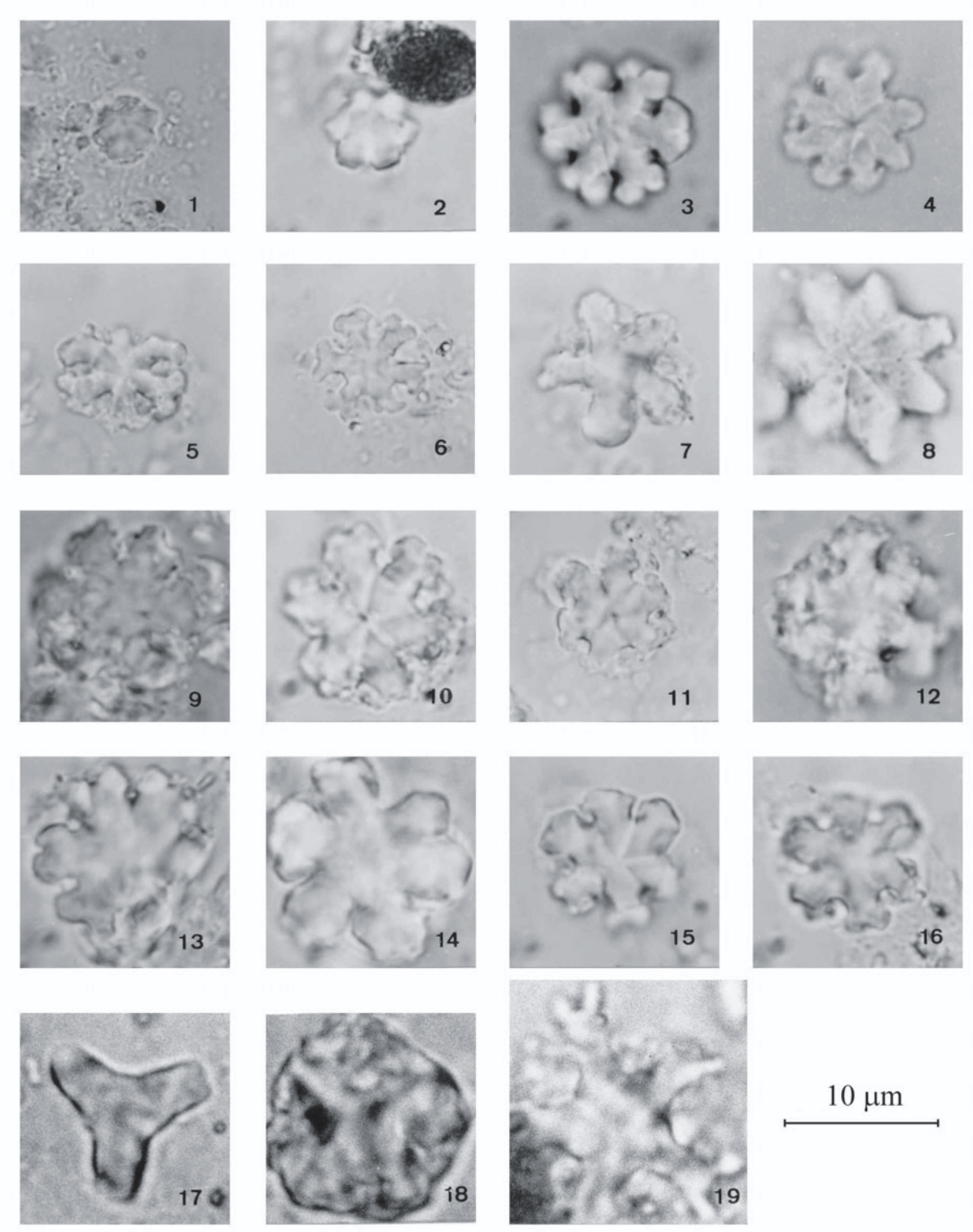

Fig. 9. LM microphotographs of calcareous nannofossil taxa from the studied sections, all pictures with parallel nicols, scale bar — 10 μm: **1–2.** *Discoaster adamanteus* Bramlette et Wilcoxon; 1 — sample F33; 2 — sample M2, section A–A'. **3.** *Discoaster deflandrei* Bramlette et Riedel, sample MI6, section E-part of Botzara syncline. **4.** *Discoaster* cf. *binodosus hirundus* Martini, sample D2, section C–C'. **5–6.** *Discoaster pansus* (Bukry et Percival) Bukry, sample M48, section A–A'. **7.** *Discoaster* sp. 1, sample M48, section A–A'. **8.** *Discoaster* sp. 2, sample FL7, section E-part of Botzara syncline. **9, 12.** *Discoaster* sp. aff. *calculosus* Bukry; 9 — sample M25, section A–A'; 12 — sample MI1, section E-part of Botzara syncline. **10–11.** *Discoaster calculosus* Bukry; 10 — sample F33; 11 — sample M25, section A–A'. **13.** *Discoaster* intermediate between *D. calculosus* and *D. deflandrei*, sample M42, section A–A'. **14.** *Discoaster* sp. aff. *deflandrei*, sample MI6, section E-part of Botzara syncline. **15–16.** *Discoaster deflandrei* Bramlette et Riedel, sample M42, section A–A'. **17.** *Rhomboaster orthostylus* (Shamrai) Bybel et Self-Trail, sample P5, section B–B', reworked from the Lower Eocene. **18.** *Nannotetrina cristata* (Martini) Perch-Nielsen, sample D2, section C–C'. **19.** *Discoaster tanii ornatus* Bramlette et Wilcoxon, sample F23, section A–A'.

diverse throughout the sections studied. Martini's (1970) zonal scheme was applied for biostratigraphic correlation of the sections. Some of zonal marker species are present; however, the scarcity or absence of others made biostratigraphic subdivisions difficult. Seven nannofossil biostratigraphic units were recognized — two in the Middle and Upper Eocene (NP16, NP17–20), one in the Lower Oligocene (NP21), one in the Upper Oligocene (NP24–25), two in the Lower Miocene (NN1, NN2–3) and one in the Middle Miocene (NN7). The presence of the Upper Miocene NN8–12 zones is questionable in the section A–A'. These age data indicate that the Pindos foredeep, as a result of Pindos thrust activity, began subsiding during the Middle Eocene. The basin was filled by submarine fan deposits until the Middle (Late?) Miocene when thrusting ended sedimentation.

Acknowledgments: The authors would like to dedicate this work to the memory of the recently deceased Prof. Vassil Vuchev — an outstanding Bulgarian geologist, who made the scientific connection between the Greek and Bulgarian researchers. The paper profited from thorough review and useful suggestions by Ján Soták and two anonymous referees.

Appendix

List of calcareous nannofossil species mentioned in the paper

A list of calcareous nannofossil taxa determined is given here. Figs. 7–9 illustrate some significant markers and other species of the nannofossil assemblages, observed during the present study (scale bar — 10 μm).

Braarudosphaera bigelowii (Gran et Braarud, 1935) Deflandre (1947)
Chiasmolithus bidens (Bramlette et Sullivan, 1961) Hay et Mohler (1967)
Chiasmolithus consuetus (Bramlette et Sullivan, 1961) Hay et Mohler (1961)
Chiasmolithus expansus (Bramlette et Sullivan, 1961) Gartner (1970)
Chiasmolithus gigas (Bramlette et Sullivan, 1961) Radomski (1968)
Chiasmolithus grandis (Bramlette et Riedel, 1954) Radomski (1968)
Chiasmolithus modestus Perch-Nielsen (1971)
Chiasmolithus solitus (Bramlette et Sullivan, 1961) Locker (1968)
Chiphragmalithus calatus Bramlette et Sullivan (1961)
Coccolithus pelagicus (Wallich, 1877) Schiller (1930)
Coccolithus miopelagicus Bukry (1971)
Cribrocentrum reticulatum (Gartner et Smith, 1967) Perch-Nielsen (1971)
Cruciplacolithus tenuis (Stradner, 1961) Hay et Mohler (1967)
Cyclicargolithus abisectus (Muller, 1970) Wise (1973)
Cyclicargolithus floridanus (Roth et Hay, 1967) Bukry (1971)
Dictyococcites bisectus (Hay, Mohler et Wade, 1966) Bukry et Percival (1971)
Dictyococcites scrippsae Bukry et Percival (1971)
Discoaster adamanteus Bramlette et Wilcoxon (1967)
Discoaster barbadiensis Tan (1927)
Discoaster bifax Bukry (1971)
Discoaster binodosus Martini (1958)
Discoaster calculosus Bukry (1971)
Discoaster deflandrei Bramlette et Riedel (1954)
Discoaster delicatus Bramlette et Sullivan (1961)
Discoaster elegans Bramlette et Sullivan (1961)
Discoaster exilis Martini et Bramlette (1963)
Discoaster kuepperi Stradner (1959)
Discoaster kugleri Martini et Bramlette (1963)
Discoaster lenticularis Bramlette et Sullivan (1961)
Discoaster lodoensis Bramlette et Riedel (1954)
Discoaster multiradiatus Bramlette et Riedel (1954)
Discoaster nodifer (Bramlette et Riedel, 1954) Bukry (1973)
Discoaster pansus (Bukry et Percival, 1971) Bukry (1973)
Discoaster saipanensis Bramlette et Riedel (1954)
Discoaster sublodoensis Bramlette et Sullivan (1961)
Discoaster tanii Bramlette et Riedel (1954)
Discoaster tanii ornatus Bramlette et Wilcoxon (1967)
Discoaster variabilis Martini et Bramlette (1963)
Ericsonia formosa (Kamptner, 1963) Haq (1971)
Ericsonia subdisticha (Roth et Hay, 1967) Roth (1969)
Helicosphaera bramlettei Muller (1970)
Helicosphaera compacta Bramlette et Wilcoxon (1967)
Helicosphaera euphratis Haq (1966)
Helicosphaera intermedia Martini (1965)
Helicosphaera lophota Bramlette et Sullivan (1961)
Helicosphaera mediterranea Muller (1981)
Helicosphaera obliqua Bramlette et Wilcoxon (1967)
Helicosphaera recta Haq (1966)
Helicosphaera scissura Miller (1981)
Helicosphaera seminulum Bramlette et Sullivan (1961)
Micula decussata Vekshina (1959)
Nannotetrina fulgens (Stradner, 1960) Achuthan et Stradner (1969)
Nannotetrina cristata (Martini, 1958) Perch-Nielsen (1971)
Prediscosphaera cretacea (Arkhangelsky, 1912) Gartner (1968)
Prinsius dimorphosus (Perch-Nielsen, 1969) Perch-Nielsen (1977)
Prinsius martinii (Perch-Nielsen, 1969) Haq (1971)
Reticulofenestra dictyoda (Deflandre, 1954) Stradner (1968)
Reticulofenestra hillae Bukry et Percival (1971)
Reticulofenestra oamaruensis (Deflandre, 1954) Stradner (1968)
Reticulofenestra pseudoumbilica (Gartner, 1967) Gartner, (1969)
Reticulofenestra umbilica (Levin, 1965) Martini et Ritzkowski (1968)
Rhomboaster contortus (Stradner, 1958) Bybell et Self-Trail (1995)
Rhomboaster orthostylus (Shamrai, 1963) Bybell et Self-Trail (1995)
Sphenolithus belemnos Bramlette et Wilcoxon (1967)
Sphenolithus capricornutus Bukry et Percival (1971)
Sphenolithus compactus Backman (1980)
Sphenolithus conicus Bukry (1971)
Sphenolithus editus Perch-Nielsen (1978)
Sphenolithus moriformis (Bronnimann et Stradner, 1960) Bramlette et Wilcoxon (1967)
Sphenolithus radians Deflandre (1952)
Sphenolithus pseudoradians Bramlette et Wilcoxon (1967)
Toweius gammation (Bramlette et Sullivan, 1961) Romein (1979)
Toweius eminens (Bramlette et Sullivan, 1961) Perch-Nielsen (1971)
Zygrhablithus bijugatus (Deflandre, 1954) Deflandre (1959)

References

Alexander J., Nichols G.J. & Leigh S. 1990: The origins of marine conglomerates in the Pindos foreland basin, Greece. *Sed. Geol.* 66, 243–254.

Aubouin J. 1965: Geosynclines. *Elsevier,* Amsterdam, 1–350.

Aubry M.P. 1984: Handbook of Cenozoic Calcareous Nannoplankton. Book 1: Ortholithae (Discoasters). *Micropal. Press, Amer. Mus. Nat. Hist.,* N.Y., 1–266.

Aubry M.P. 1988: Handbook of Cenozoic Calcareous Nannoplankton. Book 2: Ortholithae (Catinasters, Ceratoliths, Rhabdoliths). *Micropal. Press, Amer. Mus. Nat. Hist.,* N.Y., 1–279.

Aubry M.P. 1989: Handbook of Cenozoic Calcareous Nannoplankton. Book 3: Ortholithae (Pentaliths and others) Heliolithae (Fasciculiths, Sphenoliths and others). *Micropal. Press, Amer. Mus. Nat. Hist.,* N.Y., 1–79.

Aubry M.P. 1990: Handbook of Cenozoic Calcareous Nannoplankton. Book 4: Heliolithae (Helicoliths, Cribriliths, Lopa-

doliths and others). *Micropal. Press, Amer. Mus. Nat. Hist.,* N.Y., 1–381.

Avramidis P. & Kontopoulos N. 1998: Hydraulic determination and palaeoflow trends of turbidite deposits in Klematia-Paramythia basin. *Bull. Geol. Soc. Greece* 32, 2, 165–173.

Avramidis P. & Zelilidis A. 1998: Two different submarine fan lobe types and their relationship to basin evolution; implication to hydrocarbon reservoirs, western Greece. *Bull. Geol. Soc. Greece* 32, 2, 299–307.

Avramidis P., Zelilidis A. & Kontopoulos N. 2000: Thrust dissection control of deep-water clastic dispersal patterns in the Klematia-Paramythia Foreland Basin, Western Greece. *Geol. Mag.* 137, 667–685.

Avramidis P. & Kontopoulos N. 2001: Clay minerals distribution, illite crystallinity and Tmax Rock-Eval pyrolysis of turbidite deposits in Klematia-Paramythia basin, in relation to Pindos foreland evolution, western Greece. *GAIA* 16, 59–69.

Avramidis P. & Zelilidis A. 2001: The nature of deep-marine sedimentation and palaeocurrent directions as evidence of Pindos foreland basin fill conditions. *Episodes* 24, 4, 252–256.

Avramidis P., Zelilidis A., Vakalas I. & Kontopoulos N. 2002: Interactions between tectonic activity and eustatic sea-level changes in the Pindos and Mesohellenic Basins, NW Greece: basin evolution and hydrocarbon potential. *J. Petroleum Geol.* 25, 1, 53–82.

Bellas S. 1997: Calcareous nannofossils of the Tertiary Flysch (Post Eocene to Early Miocene of the Ionian Zone in Epirus, NW-Greece): Taxonomy and biostratigraphical correlations. *PhD thesis, Freie Universität Berlin*, 1–190.

Bramlette M.N. & Sullivan F.R. 1961: Coccolithophorids and related nannoplankton of the early Tertiary in California. *Micropaleontology* 7, 129–188.

Bramlette M.N. & Wilcoxon J.A. 1967: Middle Tertiary calcareous nannoplankton of the Cipero section, Trinidad, W. I. *Tulane Studies Geol.* 5, 93–131.

British Petroleum Co. Ltd. (B.P.) 1971: The geological results of petroleum exploration in western Greece. *Institute for Geology and Subsurface Research, Special report* 10, Athens.

Clews J. 1989: Structural controls on basin evolution: Neogene to Quaternary of the Ionian zone of western Greece. *Journal of the Geological Society London* 146, 447–457.

Faupl P., Pavlopoulos A. & Migiros G. 1998: On the provenance of flysch deposits in the external Hellenides of mainland Greece: results from heavy mineral studies. *Geol. Mag.* 135, 3, 412–442.

Fleury J.J. 1980: Les zones de Gavrovo-Tripolitza et du Pinde-Olonus (Grèce occidentale et Péloponnese du Nord): evolution d'une plateforme et d'une bassin dans leur cadre alpin. *Spec. Publ. Soc. Geol. du Nord* 4, 1–473.

Institute for Geology Subsurface Research of Greece & Institute Francais de Pétrole 1966: Etude geologíque de l'Epire. *Technip,* Paris.

Leigh S. & Hartley A.J. 1992: Mega-debris flow deposits from the Oligo-Miocene Pindos foreland basin, western mainland Greece: implication for transport mechanisms in ancient deep marine basins. *Sedimentology* 39, 1003–1012.

Martini E. 1971: Standard Tertiary and Quaternary calcareous nannoplankton zonation. In: Farinacci A. (Ed.): Proceedings 2nd Planktonic Conference, Roma, 1970. *Edizioni Tecnoscienza,* Rome 2, 739–785.

Mutti E. & Ricci Lucchi F. 1972: Turbidites of the northern Apennines — introduction to facies analysis. (Transl. T.H. Nilsen 1978). *Int. Geol. Rev.* 20, 125–166.

Mutti E. & Ricci Lucchi F. 1975: Turbidite facies and facies associations. In: Mutti E., Parea G.C., Ricci Lucchi F., Sagri M., Zanzucchi G., Ghibaudo G. & Saccarino (Eds.): Examples of turbidite facies and facies associations from selected formations of the northern Apennines. *I.A.S. fieldtrip guidebook A-11, International Sedimentologic Congress* IX, 21–36.

Perch-Nielsen K. 1985: Mesozoic calcareous nannofossils. Cenozoic calcareous nanno-fossils. In: Bolli H. et al. (Eds.): Plankton Stratigraphy. *Cambridge University Press,* Cambridge, 327–554.

Piper D.J.W., Panagos A.G. & Pe-Piper G.G. 1978: Conglomeratic Miocene flysch, western Greece. *J. Sed. Petrology* 48, 1, 117–126.

Underhill J.R. 1989: Late Cenozoic deformation of the Hellenide foreland, western Greece. *Geol. Soc. Amer. Bull.* 101, 613–634.

Walker R.G. 1978: Deep-water sandstone facies and ancient submarine fans: models for exploration for stratigraphic traps. *Amer. Assoc. Petrol. Geol. Bull.* 62, 932–966.

Wilpshaar M. 1995: Applicability of dinoflagellate cyst stratigraphy to the analyses of passive and active tectonic settings. *PhD thesis, University of Utrecht,* Netherlands, 1–132.

Zelilidis A., Kontopoulos N., Avramidis P. & Piper D.J.W. 1998: Tectonic and sedimentological evolution of the Pliocene-Quaternary basins of Zakynthos island, Greece: case study of the transition from compressional to extensional tectonics. *Basin Res.* 10, 4, 393–408.